SAARC J. Agric., 24(1): 249-269 (2026) *DOI: https://doi.org/10.3329/sja.v24i1.89642*

SAARC Journal of Agriculture
Journal Homage: https://www.banglajol.info/index.php/SJA

Remote Sensing-Based Spatiotemporal Assessment of Agricultural Drought in Ampara District, Sri Lanka using Google Earth Engine

S. Sawjanya[1] and M. H. F. Nuskiya[2*]

[1] Department of Geography, University of Sri Jayewardenepura, Nugegoda, Sri Lanka
[2]Department of Geography, South Eastern University of Sri Lanka, Oluvil, Sri Lanka

Abstract

Agricultural drought is a significant environmental problem affecting the yield, water resources, and human health, particularly in climate-sensitive regions. This study analyses the spatio-temporal changes of agricultural drought in Ampara District, Sri Lanka, using remote sensing indices in the Google Earth Engine (GEE) platform. Remote sensing indicators such as the Normalized Difference Vegetation Index (NDVI) and Land Surface Temperature (LST) were used to derive the Vegetation Condition Index (VCI) and Temperature Condition Index (TCI) to calculate the Vegetation Health Index (VHI), which is the major indicator of agricultural drought. The Standardized Precipitation Index (SPI) and Precipitation Condition Index (PCI) were used to measure meteorological drought. The analysis was conducted for the period 2016–2025, and the drought conditions display considerable spatial and temporal variability. There is an overall increase in Land Surface Temperature (LST) and a decrease in vegetation health, particularly since 2020, with large areas under moderate to extreme drought conditions. The VHI showed a consistent increase in the area under extreme drought conditions. Conversely, the area under no-drought conditions declined over the study period. Meteorological indices (SPI and PCI) indicate variable precipitation patterns and frequent moisture deficits, which have an impact on vegetation. The significant positive correlation (R^2=0.96-0.99) between VHI and SPI confirms the effect of rainfall on vegetation. This research reveals the Ampara District to be facing an emerging agricultural drought largely due to increased temperatures and highly variable rainfall. This study demonstrates the potential of combining remote sensing and cloud-based

[*] Corresponding author: nuskiyahassan@seu.ac.lk

Received: 29.04.2026 *Accepted: 30.06.2026*

geospatial analysis for effective drought monitoring, supporting informed decision-making for sustainable drought management and agricultural development.

Keywords: Agricultural Drought, Ampara District, Google Earth Engine, Remote Sensing, Vegetation Health Index

Introduction

Drought is a complex and periodic climatic phenomenon that impacts environmental, social, and economic systems. It is usually characterized by a prolonged reduction in rainfall, causing water shortage and impacts on vegetation and ecosystems (Mishra & Singh, 2010). Among the various types, agricultural drought is one of the most critical as it impacts soil moisture and crop production, affecting food security and economies (Dai, 2011). Droughts are frequently associated with climate variability, rising temperatures, and irregular rainfall patterns, which compound the stress on vegetation and soil health (Trenberth et al., 2014). In recent years, droughts have become increasingly common in tropical regions such as Sri Lanka in recent years due to monsoon changes and rainfall variability. These changes have resulted in significant socio-economic effects, particularly in rain-fed and irrigated agricultural zones, such as the Eastern Province, where livelihoods are highly dependent on agriculture (Eriyagama et al., 2010). Agricultural droughts affect not only crop production but also water resources, jobs, and economic growth (Vicente-Serrano et al., 2012). Therefore, drought monitoring and assessment play a vital role in drought management. Geospatial and remote sensing technologies allow effective monitoring of drought at various spatial and temporal scales. In particular, cloud computing technologies such as Google Earth Engine (GEE) allow the analysis of large volumes of satellite data, making it well-suited for drought monitoring (Gorelick et al., 2017). Using satellite data products such as Landsat 8, Sentinel-2, and precipitation data, a range of drought indices can be calculated to assess vegetation status and climatic changes. These include the Normalized Difference Vegetation Index (NDVI) and Land Surface Temperature (LST), which are widely used to measure vegetation status and temperature anomalies, respectively (Zhang et al., 2013). Moreover, the Vegetation Condition Index (VCI) and Temperature Condition Index (TCI) are derived from NDVI and LST and measure vegetation condition and temperature anomalies, respectively. These are combined to calculate the Vegetation Health Index (VHI), a useful index for the assessment of agricultural drought by considering vegetation and temperature conditions (Kogan, 2001). Furthermore, meteorological-based indices, such as the Standardized Precipitation Index (SPI) and Precipitation Condition Index (PCI), are considered to understand rainfall anomalies and their impact on drought (McKee et al., 1993; Guttman, 1999).

Agricultural drought is an important environmental stress factor that affects crop production, water resources, and food security in semi-arid and dry zones, such as Sri

Lanka's Ampara District. The combination of satellite remote sensing and cloud geospatial technologies has improved drought monitoring in recent years through spatiotemporal monitoring of vegetation and moisture indices in real time. For instance, remotely sensed drought indices, such as the Integrated Drought Severity Index (IDSI), have been applied to monitor agricultural drought in Sri Lanka, revealing vulnerability in districts like Ampara (Alahacoon & Amarnath, 2022). Similarly, the integration of multiple satellite datasets has demonstrated the potential to capture drought variability and its effects on hydrologic and agricultural drought impacts (Srimali et al., 2025). The development of GEE has also improved large-scale drought monitoring by enabling effective processing of multi-temporal satellite data and machine learning classification techniques (Fernando & Senanayake, 2024). Research also indicates that the integration of remote sensing indices with long-term time series data enhances the ability to capture drought patterns and their spatial variability, leading to better decision-making processes (Imtiaz et al., 2025). Recent studies focusing on remote sensing-derived vegetation indices have demonstrated their potential for monitoring environmental dynamics, including urban vegetation changes in Colombo District, Sri Lanka, using Sentinel-2 data (Zahir et al., 2024). These vegetation studies are complemented using geospatial technologies (integrated with machine learning and OpenStreetMap) in GEE for disaster risk reduction and spatial analysis in Sri Lanka, showcasing the platform's potential for environmental monitoring (Iyoob et al., 2025). Additionally, long-term geospatial analyses have established the effectiveness of remote sensing and GIS methods to study spatiotemporal land and forest cover changes in the dry zone of Sri Lanka (Ranagalage et al., 2020; Walawe Durage, 2023). However, there is limited research on high-resolution and localized agricultural drought monitoring that integrates multiple remote sensing indices within cloud-computing platforms, such as Google Earth Engine (GEE), for districts such as Ampara. Therefore, further spatiotemporal investigations are needed. In this study, the Ampara District in the Eastern Province of Sri Lanka is chosen as the study region, which has shown significant changes in rainfall variability, increasing temperature, and decreasing vegetation in recent years. This suggests the risk of agricultural drought is increasing. Hence, this research aims to understand the spatial and temporal dynamics of agricultural drought through the analysis of remote sensing indices, calculated using the Google Earth Engine platform. This is then validated against the meteorological drought indices to assess the relationship between rainfall and vegetation. The trend analysis, from 2016 to 2025, shows variations in drought. This study provides information on the drought and identifies drought-prone areas in the region. This information is essential for decision-making, planning, and management of drought and water resources and sustainable agriculture in Ampara.

Methodology

Study Area

This research was carried out in the Ampara District in the southeast of Sri Lanka. The study area is roughly located between 7°00′ and 7°45′ North latitude and between 81°00′ and 81°55′ East longitude. The Ampara District covers an area of about 4,415 sq. km and is one of the major districts in Sri Lanka. The Ampara District is in the Eastern Province of Sri Lanka and is bounded by Batticaloa District in the north, Monaragala District in the west, and the Indian Ocean in the east (Department of Census and Statistics, 2023). The topography of the region is predominantly flat to gently undulating lowlands with altitudes ranging from sea level to 150 m above mean sea level. The district is located in the dry zone of Sri Lanka with a rainfall range of 1,200 mm to 1,900 mm per year, and is greatly influenced by the Northeast monsoon (World Bank, 2021). The major water source in the region is the Gal Oya River, which irrigates the Senanayake Samudra reservoir, which is a major water resource for irrigation (Irrigation Department of Sri Lanka, 2022). The dominant soil types of the region are reddish-brown earth, alluvial, and sandy soils, which are very fertile for agriculture (FAO, 2020). Agriculture is the main land use in the region, with paddy, maize, sugarcane, pulses, plantation crops (coconut, fruits), and other minor crops. However, it is highly sensitive to climate change, drought, and water scarcity, which adversely impact agriculture (Department of Census and Statistics, 2023).

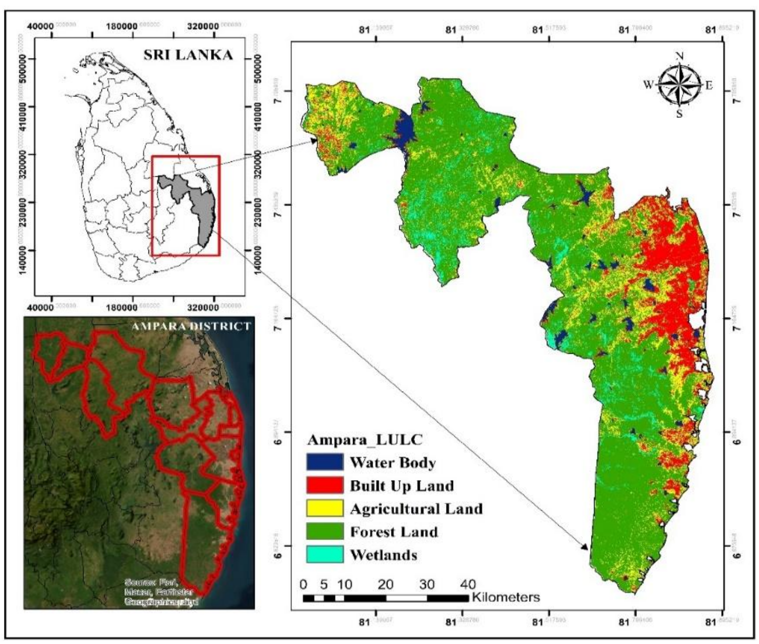

Fig. 1. Study Location & Land Use/Land Cover

Land Use / Land Cover (LULC)

The Land Use/Land Cover (LULC) mapping of the Ampara region was carried out using a Support Vector Machine (SVM) classifier in the Google Earth Engine (GEE) platform. The study area is classified into five broad classes: Water, Built-up, Agriculture, Forest, and Wetlands. The results showed that agriculture was the dominant land use class, which occupies a large portion of the study region in the central and eastern regions. This is mostly used for rice and reservoir - irrigated farming. The forest region is mainly located in the western and northwest parts, which are mainly natural vegetation and forest reserves (Survey Department of Sri Lanka, 2022). The built-up area is mainly concentrated along the coastal region of the eastern belt and urban settlements such as Ampara and Kalmunai, depicting urbanization. The wetlands are located in depressions and near water sources, playing a vital role in the ecosystem and biodiversity. The water bodies (reservoirs, tanks, and river network) are widely distributed throughout the study area, with a high concentration around irrigation structures such as Senanayake Samudra (Irrigation Department of Sri Lanka, 2022). In summary, the LULC analysis indicated that although agriculture remained the dominant land use category, increasing urbanization and localized reductions in forest cover were observed within the study area. This change, along with climatic conditions, plays a role in the vulnerability to agricultural drought and environmental degradation in the Ampara region (FAO, 2020; World Bank, 2021).

Materials and Methods

Satellite-Based Drought Indices

In this study, all drought indices were calculated using remote sensing data products in the Google Earth Engine (GEE) platform. Land surface optical and thermal data products of Landsat 8 OLI/TIRS Surface Reflectance Tier 1 were used to calculate the Normalized Difference Vegetation Index (NDVI) and Land Surface Temperature (LST) with the formulas given in Table 1. They were indicators of vegetation health and surface temperature conditions, respectively, in response to drought. The time-series NDVI and LST were used to calculate the Vegetation Condition Index (VCI) and the Temperature Condition Index (TCI). These represented vegetation stress and temperature anomalies, respectively, and are categorized into various levels of drought conditions. The combined use of VCI and TCI produced the Vegetation Health Index (VHI), which is taken as the main indicator to assess agricultural drought in the study region. In this study, VHI was calculated for the period 2016-2025 to study the long-term drought patterns. To study meteorological drought, the Precipitation Condition Index (PCI) was calculated using satellite-based precipitation data from TRMM (Tropical Rainfall Measuring Mission) 3B42/3B43. The Standardized Precipitation Index (SPI) was also computed using rainfall observations from relevant meteorological agencies in Sri Lanka. The SPI is used to standardise precipitation variations. Moreover, land use/land cover (LULC) classification of the study region was performed using Copernicus Global Land Cover Layers (CGLS-

LC100 Collection 3) in the GEE platform. This mapping was useful for understanding the distribution of different land cover types and their association with drought.

Table 1. Drought Indices Utilized for the Study

Indices	Formula	Source
SPI	$\frac{(X_{ij}-X_{im})}{\sigma}$	Naresh Kumar et al., 2009
NDVI	$\frac{(NIR-Red)}{(NIR+Red)}$	Kogan et al., 2003; Venkatesh et al., 2022
LST	1. Digital Numbers to spectral radiance $L_\lambda = ML \times Q_{cal} + AL$ 2. Spectral radiance to brightness temperature $BT = \frac{K2}{\ln(\frac{K1}{L_\lambda}+1)} - 273.15$ 3. Proportion of Vegetation $PV = \left(\frac{NDVI - NDVI_{min}}{NDVI_{max} - NDVI_{min}}\right)^2$ 4. Land Surface Emissivity $LSE = 0.004 \times PV + 0.986$ 5. Land Surface Temperature $LST = \frac{BT}{1 + W \times \left(\frac{BT}{14380}\right) \times \ln(LSE)}$	Sun & Kafatos, 2007; Mustafa et al., 2020; Anbazhagan, S., & Paramasivam, 2016
VCI	$\frac{NDVI - NDVI_{min}}{NDVI_{max} - NDVI_{min}}$	Kogan et al., 2003
TCI	$\frac{LST_{max} - LST}{LST_{max} - LST_{min}}$	Seiler et al., 1998; Zhou et al., 2019
PCI	$\frac{TRMM - TRMM_{min}}{TRMM_{max} - TRMM_{min}}$	Meza et al., 2025; Zhang et al., 2022
VHI	$\alpha \times VCI + (1-\alpha) \times TCI$	Sun et al., 2022

3.2 Earth Engine Data Processing

Google Earth Engine (GEE) is a cloud-computing platform for geospatial data processing that allows efficient processing of massive satellite data. In this research, the data processing and analysis were performed with the GEE JavaScript API, enabling fast calculation and visualization of drought indices at large scales (Gorelick et al., 2017). The necessary data were downloaded from the GEE data catalogue using the ee. Image Collection framework. These include using several built-in functions, such as filter date, filter Bounds, map, reduce, clip, expression and Export, to preprocess, filter, and analyze satellite imagery. These functions help in temporal filtering and clipping the images to the study area, computing indices, and exporting the images for analysis. To map agricultural drought, annual NDVI and LST images were created for the years 2016-2025. Annual minimum and maximum NDVI and LST values were used to calculate the VCI and TCI, respectively. Finally, the VHI was calculated as a combination of VCI and TCI, which gives an overall assessment of vegetation status and drought. To assess the meteorological drought, SPI was computed based on long-term rainfall, and PCI was computed from satellite precipitation data for the same period. The calculated indices were then spatially and temporally analyzed to detect drought-prone regions and trends. The computed outputs were exported from GEE with the same spatial resolution, projection, and scale. These were also visualized and mapped to study the spatial and temporal distribution of drought severity in the Ampara region. Figure 2. (Methodological Flowchart) shows the methodological approach followed in this study.

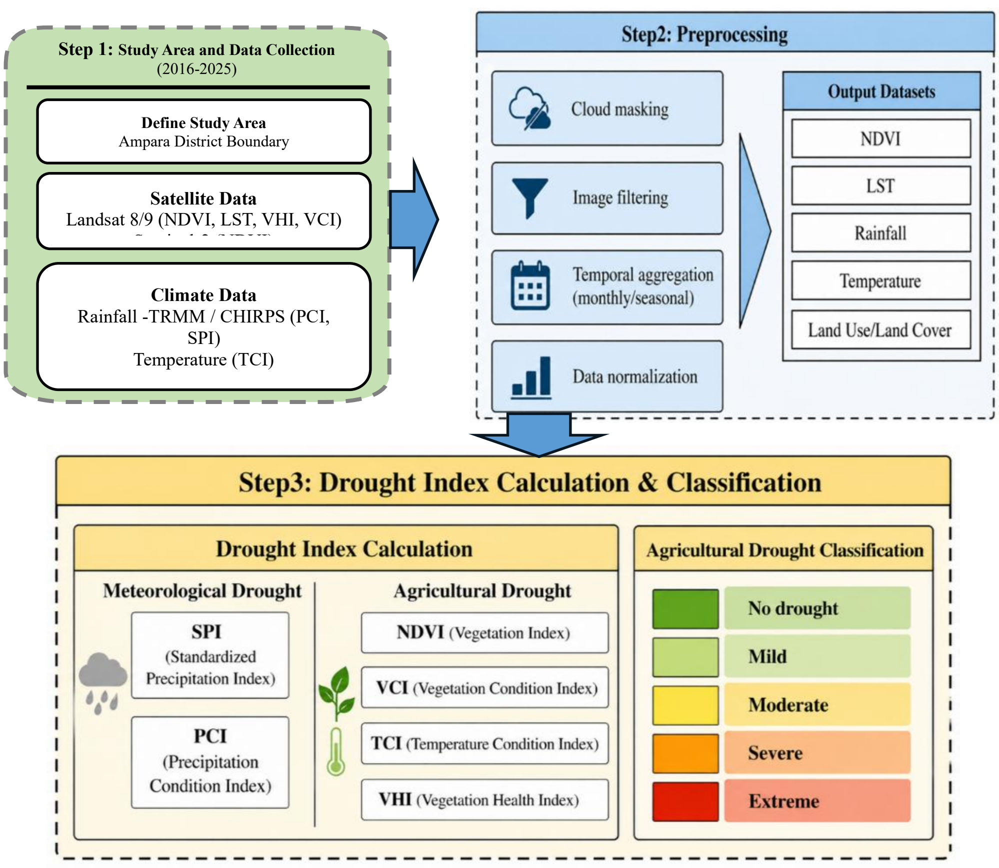

Fig. 2. Methodological Framework for Agricultural Drought Assessment

Results and Discussion

The agricultural drought status of the Ampara region has been analyzed using the Vegetation Health Index (VHI) with a combination of two indices: Temperature Condition Index (TCI) and Vegetation Condition Index (VCI). These indices are calculated using Land Surface Temperature (LST) and Normalized Difference Vegetation Index (NDVI). In addition, the agricultural drought is compared with the meteorological drought indices such as the Precipitation Condition Index (PCI) and the Standardized Precipitation Index (SPI). All the indices were computed and interpreted using Google Earth Engine (GEE) for the duration of 2016-2025.

Land Surface Temperature (LST)

Land Surface Temperature (LST) is an important factor in detecting agricultural drought because of its impact on vegetation. The annual LST for the years 2016 - 2025 was categorized into five classes: very low (<25°C), low (25-28°C), moderate (28-31°C), high (31-34°C), and very high (>34°C). The spatial distribution showed that the moderate to high LST (28-34°C) was dominant in the Ampara region over the years. In particular, the years 2020 and 2022 show the highest temperature intensities with a maximum value of 36.41°C and 34.63°C, respectively. Eastern and southeastern coastal areas showed consistently high temperatures, suggesting a higher drought stress. By contrast, cooler temperatures were observed in the inland vegetated areas in some years, particularly in 2016 and 2018, with minimum values ranging from 24.76°C to 27.70°C. Over time, the upward trend of LST indicated an increase in thermal stress, which has a profound impact on crop yield reduction during agricultural drought.

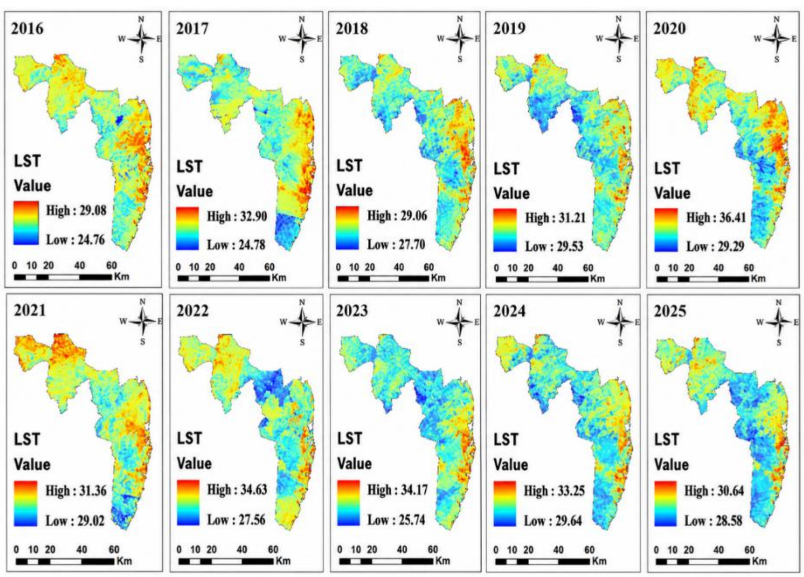

Fig. 3. Annual Land Surface Temperature from 2016 to 2025

Normalized Difference Vegetation Index (NDVI)

The NDVI is an indicator of vegetation cover and health, with values ranging from -0.11 to 0.53 in the region. The NDVI values were classified into six categories: bare soil/water (<0), very low (0- 0.2), low (0.2- 0.4), moderate (0.4- 0.6), high (0.6-0.8), and very high (>0.8). The results showed that the low classes (0.2 - 0.4 and 0 - 0.2) of the NDVI are the most prominent in the Ampara region over the years. Very high NDVI (>0.5) was restricted and occurred in small patches, which shows a small amount of healthy vegetation. The NDVI is at its lowest in 2020 and 2024 (maximum NDVI of 0.43 and 0.42) due to decreased vegetation health. While a slight improvement was observed in 2023 and 2025 (up to approximately 0.52 and 0.47, respectively), the overall vegetation condition remained poor. Spatially, the central and southeastern parts of the basin exhibited low NDVI values, suggesting poor vegetation and drought-prone areas.

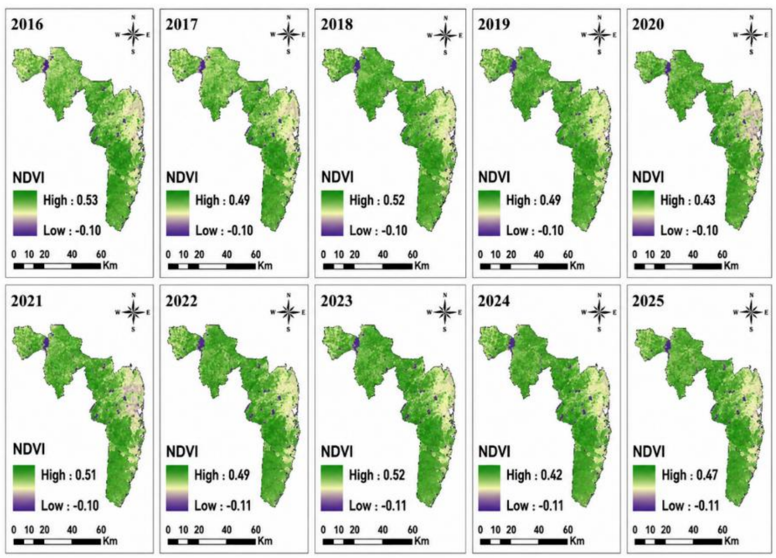

Fig. 4. Annual Normalized Difference Vegetation Index from 2016 to 2025

Temperature Condition Index (TCI)

TCI has a range of 0-100 and is classified into no drought (>40), slight drought (31-40), moderate drought (21-30), high drought (11-20), and extreme drought (<10). The TCI is inversely related to drought severity. The spatial and temporal distribution of TCI revealed a prevalence of high (11-20) and extreme drought (<10) across large areas of the study region, especially in 2022 and 2025, when large areas are covered by red color representing a high thermal stress. In contrast, 2019 showed relatively high TCI values (0-0.8 category showing less stress) and thus less drought in the region. The areas in the north and the center of the study area showed a strong presence of drought, and the regions with low drought are seen only in isolated areas.

In general, the trend of TCI values showed a decline over the years, where temperature-induced drought is increasing in Ampara.

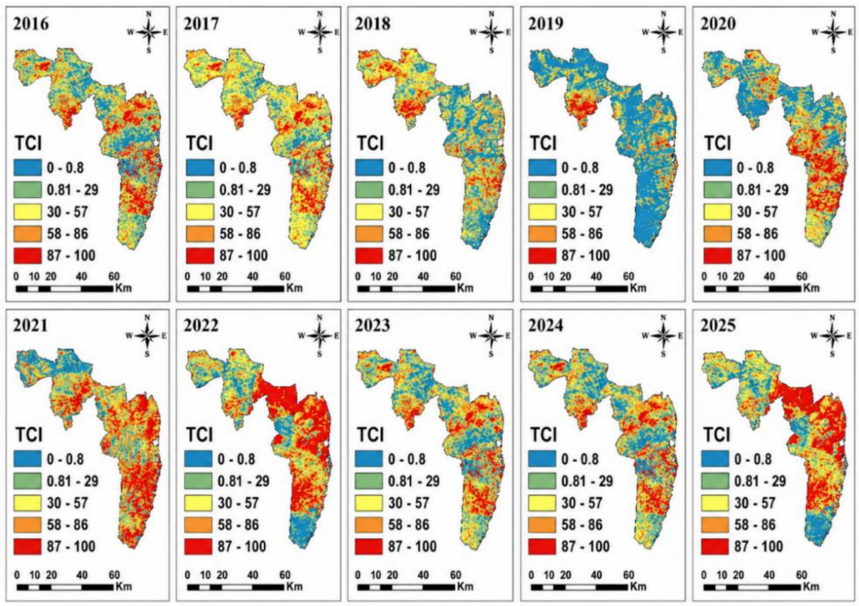

Fig. 5. Annual Temperature Condition Index of 2016 to 2025

Vegetation Condition Index (VCI)

The VCI is an important indicator of vegetation condition across the study region and helps assess drought severity. Annual VCI values were derived for the period 2016-2025. The VCI values ranged from 0-100, and were classified into five categories: extreme drought (<16), high drought (17-40), moderate drought (41-61), slight drought (62-83), and no drought (>84). The findings showed a decreasing trend in vegetation conditions, with more extreme and high drought classes after 2020. Moderate vegetation condition (41-61) is relatively prevalent in 2016-2018. In 2020 and 2022, vast areas of the region were transformed into high drought (17-40) and extreme drought conditions (<16). In 2024 and 2025, a clear recovery in vegetation was observed with moderate to slight drought (41-61) conditions occurring across many parts of the study area, suggesting improved vegetation growth. Spatially, the southeast and coastal areas were generally in poor condition. VCI was an important index when combined with other indices, such as the Temperature Condition Index (TCI), to create the Vegetation Health Index (VHI). This was useful for a better description of drought, including vegetation and temperature stress.

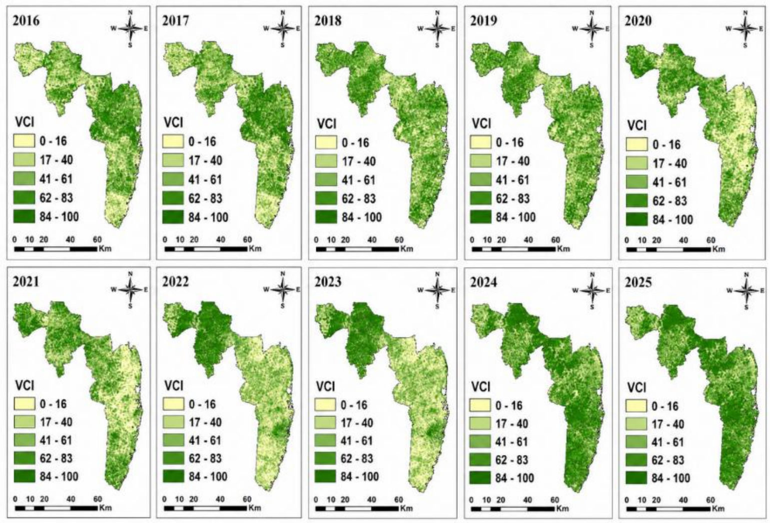

Fig. 6. Annual Vegetation Condition Index from 2016 to 2025

Vegetation Health Index (VHI)

The VHI is a combination of both TCI and VCI, ranging from 0 to 100, and can be classified as extreme drought (<30), high drought (31-47), moderate drought (48-60), slight drought (61-75), and no drought (>76).

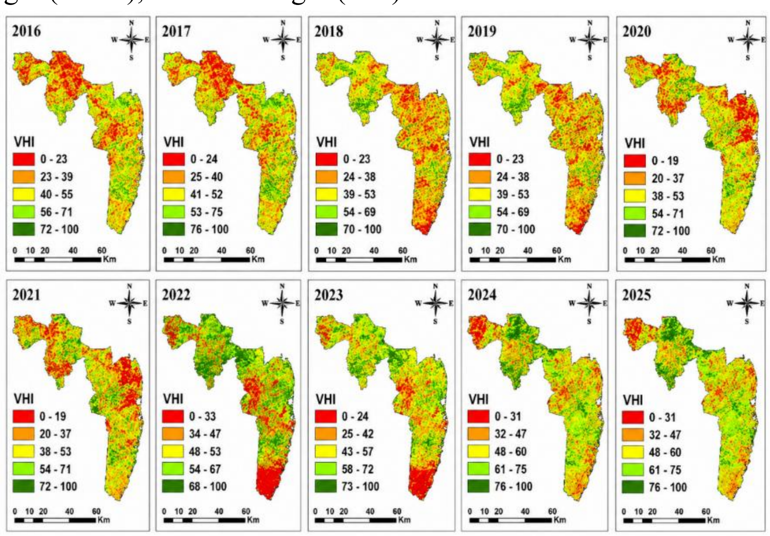

Fig. 7. Annual Vegetation Health Index of 2016 to 2025

The VHI results indicated that drought conditions intensified over the study period. During 2016–2017, vegetation health was relatively good, with most areas experiencing moderate to slight drought conditions. However, 2022 shows severe degradation, with extreme drought (<33) covering large and mostly southern and southeastern parts of the region. Moderate improvement was observed in 2023-2025; droughts continued to be prevalent. The map showed that the central and coastal areas were severely affected, with only small areas having healthy vegetation. Overall, the VHI showed an increase in vegetation stress in recent years.

Precipitation Condition Index (PCI)

The PCI values obtained in this study ranged from 0.98 to 62, reflecting the actual precipitation conditions observed during the study period. Although PCI is commonly classified on a 0–100 scale, the calculated values are dependent on local climatic variability and do not necessarily occupy the full theoretical range. The northern and central parts are often under high to extreme drought classes, while the southern and southeastern parts are infrequently under moderate precipitation classes. In 2024 and 2025, an improvement in rainfall distribution was observed, with high PCI values (44-62) covering large parts of the study area, indicating favorable rainfall conditions. However, previous years like 2018 and 2020 are characterized by lower PCI values, depicting precipitation deficits. This variable rainfall pattern played a key role in drought variability.

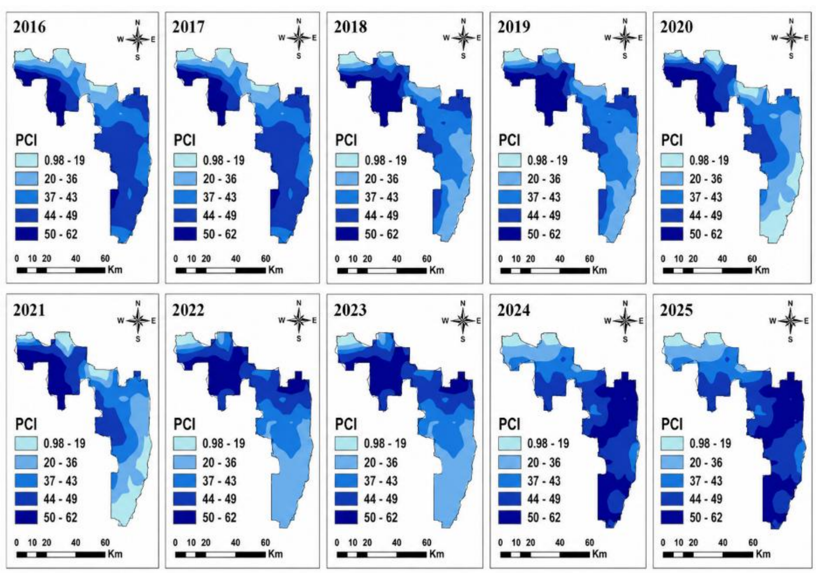

Fig.8. Annual Precipitation Condition Index of 2016 to 2025

Standardized Precipitation Index (SPI)

The SPI values are divided into seven classes from extremely dry (< -2.0) to extremely wet (≥ 2.0). The SPI results showed that the northern and central regions of the study area were under dry conditions, especially in 2016, 2018, and 2022, which were dominated by severely dry (-1.5 to -1.99) and extremely dry (≤ -2.0) classes. However, the eastern and southeastern parts of the area showed moderate to wet conditions (>0.5) in some years (2020 and 2025).

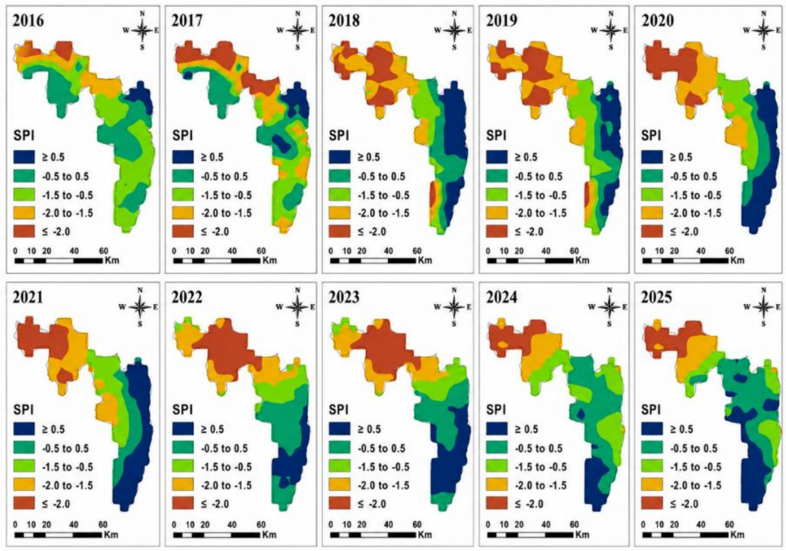

Fig. 9. Annual Standardized Precipitation Index of 2016 to 2025

The overall temporal variations show that some years have good rainfall conditions, but due to the uneven distribution of rainfall, droughts persist in many parts of the study region. The SPI findings were consistent with PCI and VHI, and indicated the occurrence of meteorological drought.

Agricultural Drought Assessment

The Ampara region's agricultural drought assessment is conducted by using agricultural and meteorological indicators. In this study, agricultural drought was analyzed in detail using the Vegetation Health Index (VHI), and meteorological drought was compared with the results of PCI and SPI. The initial examination of the LST and NDVI results showed that the study region was dominated by moderate to high temperatures and low to moderate levels of vegetation cover, suggesting vegetation stress. As such, the TCI and VCI results showed that high and extreme drought categories were more prevalent in the central and southeastern regions, while the no drought and mild drought categories were seen only in a few and isolated parts during some years. Hence, the vegetation health was not uniformly distributed, and the region was more likely to experience drought conditions. Finally, the spatial and temporal analysis of the VHI results clearly illustrated the spatial variation of drought categories for the period between 2016 and 2025. The non-drought area fluctuated from 1100 sq. km in 2016 to 1010 sq. km in 2017 and 950 sq. km in 2018, before increasing to 1000 sq. km in 2019. However, it decreased again to 900 sq. km in

2020, and gradually increased to 950 sq. km in 2021, reaching a peak of 1050 sq. km in 2022. A sharp decline was observed in 2023 (850 sq. km), followed by a gradual recovery to 950 sq. km in 2024 and 1000 sq. km in 2025.

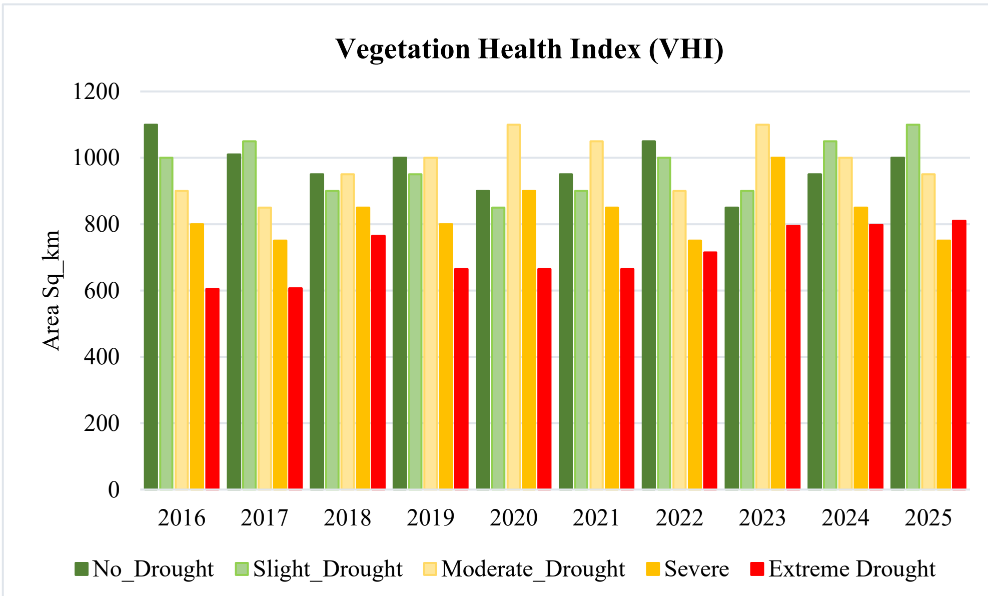

Fig. 10. Graphical representation of VHI classes for consecutive years (2016-2025)

The slight drought category also showed significant variations with values of 1000 sq. km in 2016, 1050 sq. km in 2017, then a decline to 900 sq. km in 2018 and an increase to 950 sq. km in 2019. It further declines to 850 sq. km in 2020, increases to 900 sq. km in 2021, and reaches 1000 sq. km in 2022. It decreases slightly in 2023 (900 sq. km), but increases significantly to 1050 sq. km in 2024 and the maximum of 1100 sq. km in 2025, suggesting a temporary improvement in vegetation health during the last few years. The moderate drought category exhibits an increasing and dominant pattern over the years, with 900 sq. km in 2016, 850 sq. km in 2017, and 950 sq. km in 2018. It increases further to 1000 sq. km in 2019 and reaches a peak of 1100 sq. km in 2020. Although it slightly decreases to 1050 sq. km in 2021, it drops significantly to 900 sq. km in 2022, and again rises sharply to 1100 sq. km in 2023, followed by 1000 sq. km in 2024 and 950 sq. km in 2025. This suggests that moderate drought conditions are prevalent and persistent in this area. Severe drought varies between moderate and high severity in 2016 (800 sq. km), falling to 750 sq. km in 2017, rising to 850 sq. km in 2018, and then levelling out at 800 sq. km in 2019. It rises to 900 sq. km in 2020, decreases to 850 sq. km in 2021, and further drops to 750 sq. km in 2022. However, a significant increase is observed in 2023 (1000 sq. km), followed by a decrease to 850 sq. km in 2024 and 750 sq. km in 2025.

Crucially, the class of extreme drought shows a gradual increase in the entire study period from 605 sq. km in 2016 to 607 sq. km in 2017 and subsequently to 765 sq. km in 2018. It decreases to 665 sq. km in 2019 and 2020, remains constant at 665 sq. km in 2021, and then increases to 715 sq. km in 2022, 795 sq. km in 2023, 798 sq. km in 2024, and reaches the highest value of 810 sq. km in 2025. This progressive increase clearly shows the gradual increase in the area affected by extreme drought. This clearly shows progressive environmental degradation, with the area under healthy vegetation (no drought) being unstable and partially decreasing, while the extreme drought is increasing. The mixed variation in slight, moderate, and severe drought categories also indicates the instability in vegetation condition caused by the temperature variations. This is mostly due to uneven and inadequate rainfall experienced in the Ampara region, as indicated by the results of PCI and SPI. The links between VHI, PCI, and SPI results confirmed that the years with higher drought intensity have lower rainfall and higher temperature, which impacts vegetation and crop production. The shifts towards higher proportions of moderate to extreme drought, particularly after 2020, suggested that the study region is more susceptible to agricultural drought. This could result in further losses in vegetation cover and have profound consequences for agriculture and water resources in the future.

Correlation between VHI and SPI

The values of VHI and SPI were correlated and are shown in Figure 11 (Correlation Graph). The correlation analysis was conducted for all years (2016- 2025), and the results were presented graphically. The correlation between SPI (drought) and VHI (vegetation drought) was examined to assess the effect of rainfall variability on vegetation. The correlation graphs clearly showed a strong positive correlation of the SPI and VHI values in all the years, where R^2 values (coefficient of determination) are around 0.96-0.99, which indicates a high correlation. In the graph, the different groups of points were considered as representing different drought-vegetation health conditions. The smaller SPI values (negative values such as -1.7, -1.6, -1.3) were associated with lower VHI values (30-45), representing dry conditions and poor vegetation health. Likewise, moderate SPI (such as -0.5, -0.4, -0.3, -0.2, 0.2) corresponds to moderate VHI (such as 55-70), which means moderate vegetation under slightly dry to normal climatic conditions. Positive SPI values (e.g., 0.6, 0.7, 0.9, 1.0) corresponded to higher VHI values (approximately 75-90), which represent good vegetation under wet conditions. Spatio-temporal interpretations from the correlation results indicate that in the early years (2016-2018), the correlation points are more spread out across various ranges of SPI and VHI, representing a mixture of climatic conditions with both dry (low) and moderate vegetation conditions. However, in the years 2019-2022, the correlation data points tend to be closer to the regression line in the moderate to dry SPI values (-1.0 to 0.2) and moderate VHI values (50-70). This suggests that the vegetation condition during these years is mainly affected by low precipitation.

In addition, during the period 2023-2025, the correlation was very strong, with R^2 values ranging from 0.98 to 0.99, and the data points closely followed a linear pattern. These years, while SPI values show some improvement (up to 1.0), VHI values still indicate moderate vegetation condition, implying that vegetation is still recovering, and is still vulnerable to climatic conditions. In summary, the correlation analysis demonstrated that SPI and VHI were highly correlated, meaning that reduced rainfall affects the vegetation health, thus increasing agricultural drought. The high density of correlation points in the moderate to dry SPI range and moderate VHI range indicates that the study area experiences drier conditions more often with moderate vegetation health. This correlation indicates meteorological drought is one of the main factors contributing to agricultural drought in the Ampara region. If these conditions remain for an extended period, it could result in increased vegetation stress, soil and groundwater drying, and, finally, impact crop production and sustainability.

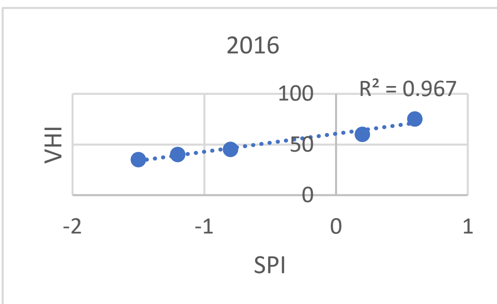

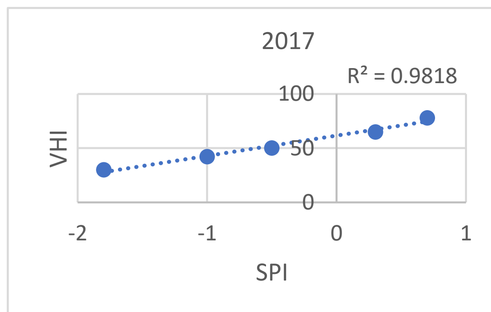

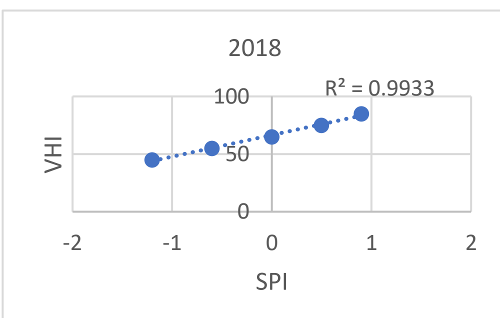

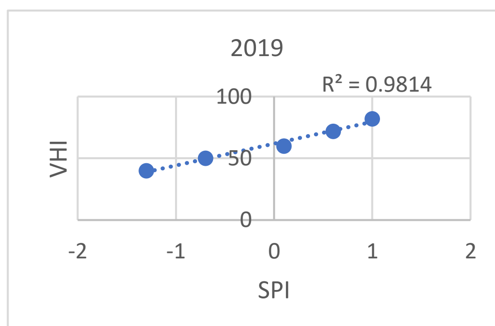

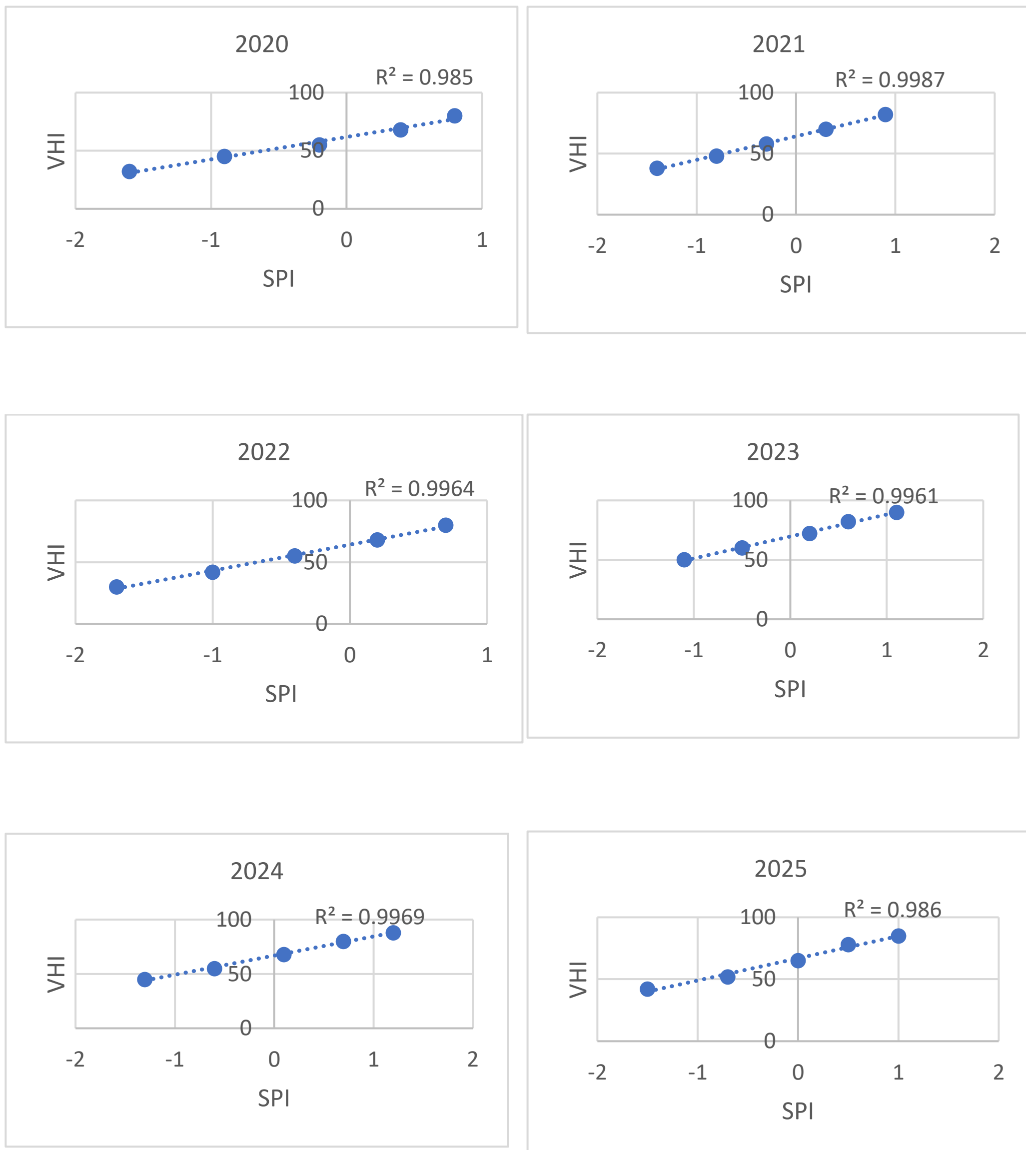

Fig. 11. Correlation between VHI and SPI for consecutive years (2016-2025)

Conclusion

The agricultural drought assessment of Ampara District was successfully conducted using the cloud-based Google Earth Engine (GEE) platform. Several remote sensing indices were calculated and mapped to analyze the spatial and temporal patterns of drought. The indices (LST, NDVI, TCI, VCI, and VHI) were computed to assess agricultural drought, while the meteorological indices (PCI and SPI) were used to analyze the effect of rainfall variability. The findings suggested that agricultural drought in the study area was greatly affected by meteorological drought, especially rainfall variability and temperature anomalies. The assessment of VHI results from 2016 to 2025 showed that the area under healthy vegetation (no drought category) fluctuated considerably, ranging from 1100 sq. km to 850 sq. km, while the extreme drought category showed a steady increase from 605 sq. km in 2016 to 810 sq. km in 2025. This suggests an increase in the extent of drought over the region. Likewise, the moderate and severe drought categories were prevalent throughout the study period, indicating persistently stressed vegetation conditions. The SPI analysis also indicates that a large region is often moderately dry and severely dry, showing the variability and lack of rainfall. Further, the correlation between the SPI and VHI shows a strong positive relationship (R^2=0.96-0.99), suggesting that vegetation health is strongly linked with rainfall. The trends of both indices confirmed that vegetation health was directly linked to rainfall, with reduced rainfall leading to a loss in vegetation cover and increased agricultural drought. In summary, the results revealed that the Ampara region was increasingly susceptible to drought, with a growing trend in extreme drought over the past few years. This could result in further loss of vegetation cover, soil moisture loss, and increased water stress. Thus, it is crucial to adopt sustainable management practices such as drought-tolerant cropping, water resource management, and climate-proof planning to reduce the impacts of future droughts and promote sustainable agricultural development in the region.

Data Availability Statement

The datasets used in this study are publicly available on the Google Earth Engine platform and in other sources cited in the manuscript. The Google Earth Engine scripts used for data processing and analysis are available from the corresponding author upon reasonable request.

References

Alahacoon, N., & Amarnath, G. (2022). Agricultural drought monitoring in Sri Lanka using multisource satellite data. *Advances in Space Research*, *69*(11), 4078-4097. https://www.sciencedirect.com/science/article/pii/S0273117722001958

Anbazhagan, S., & Paramasivam, C. R. (2016). Statistical correlation between land surface temperature (LST) and vegetation index (NDVI) using multi-temporal Landsat TM data. *International Journal of Advanced Earth Science and Engineering*, *5*(1), 333-346. https://www.academia.edu/download/55228063/409-1225-1-PB.pdf

Department of Census and Statistics. (2023). Statistical pocket book 2023: Sri Lanka. Department of Census and Statistics, *Ministry of Finance, Economic Stabilization and National Policies*. https://www.statistics.gov.lk

Dai, A. (2011). Characteristics and trends in various forms of the Palmer Drought Severity Index during 1900–2008. *Journal of Geophysical Research: Atmospheres*, *116*(D12). https://agupubs.onlinelibrary.wiley.com/doi/abs/10.1029/2010jd015541

Dissanayake, D. M. S. J. B. (2020). Multi-Decadal Forest-Cover Dynamics in the Tropical Realm: Past Trends and Policy Insights for Forest Conservation in the Dry Zone of Sri Lanka. http://repository.rjt.ac.lk/handle/123456789/3228

Domínguez-Meza, V. H., Gutiérrez, I. G., Poot-Poot, W. A., & Campanur, X. C. R. (2025). Meteorological drought using the Precipitation Condition Index in dry northeast Mexico during the 2000-2023 period. *Revista de Teledetección*, (66). https://polipapers.upv.es/index.php/raet/article/view/22885

Eriyagama, N., Smakhtin, V., Chandrapala, L., & Fernando, K. (2010). Impacts of climate change on water resources and agriculture in Sri Lanka: a review and preliminary vulnerability mapping.

Fernando, W. A. M., & Senanayake, I. P. (2024). Developing a two-decadal time-record of rice field maps using Landsat-derived multi-index image collections with a random forest classifier: A Google Earth Engine-based approach. *Information Processing in Agriculture*, *11*(2),260-275. https://www.sciencedirect.com/science/article/pii/S2214317323000197

Food and Agriculture Organization of the United Nations (FAO). (2020). *Sri Lanka: Drought impact and vulnerability assessment*. FAO Drought Portal. https://www.fao.org/in-action/drought-portal/preparedness/vulnerability-and-impact-assessment/national-case-studies/sri-lanka/en

Gorelick, N., Hancher, M., Dixon, M., Ilyushchenko, S., Thau, D., & Moore, R. (2017). Google Earth Engine: Planetary-scale geospatial analysis for everyone. *Remote sensing of Environment*, *202*, 18-27. https://www.sciencedirect.com/science/article/pii/S0034425717302900

Guttman, N. B. (1999). Accepting the standardized precipitation index: a calculation algorithm 1. *JAWRA Journal of the American Water Resources Association*, *35*(2), 311-322. https://onlinelibrary.wiley.com/doi/abs/10.1111/j.1752-1688.1999.tb03592.x

Imtiaz, F., Farooque, A. A., Randhawa, G. S., Garmdareh, S. E. H., Wang, X., Esau, T. J., ... & Sadiq, R. (2025). Remote sensing-based spatiotemporal dynamics of agricultural drought on Prince Edward Island using Google Earth Engine. *Ecological Informatics*, *86*, 103073. https://www.sciencedirect.com/science/article/pii/S1574954125000822

Irrigation Department of Sri Lanka. (2022). *Administration report 2022*. https://www.irrigation.gov.lk/web/images/Downloads/Publications/Administration_Report_2022_Part_II.pdf

Iyoob, A. L., Zahir, I. L. M., Suthakaran, S., & Fowzul Ameer, M. L. (2025, June). Machine Learning-Based Urban Nighttime Light Intensity Analysis in Sri Lanka Using VIIRS Images. In *International Conference on Innovations in Computational Intelligence and Computer Vision* (pp. 51-67). Cham: Springer Nature Switzerland. https://link.springer.com/chapter/10.1007/978-3-032-09825-2_5

Kogan, F. N. (2001). Operational space technology for global vegetation assessment. *Bulletin of the American meteorological society*, *82*(9), 1949-1964. https://journals.ametsoc.org/view/journals/bams/82/9/1520-0477_2001_082_1949_ostfgv_2_3_co_2.xml

Kogan, F., Gitelson, A., Zakarin, E., Spivak, L., & Lebed, L. (2003). AVHRR-based spectral vegetation index for quantitative assessment of vegetation state and productivity. *Photogrammetric Engineering & Remote Sensing*, *69*(8), 899-906. https://www.ingentaconnect.com/content/asprs/pers/2003/00000069/00000008/art00004

McKee, T. B., Doesken, N. J., & Kleist, J. (1993, January). The relationship of drought frequency and duration to time scales. In *Proceedings of the 8th Conference on Applied Climatology* (Vol. 17, No. 22, pp. 179-183). https://climate.colostate.edu/pdfs/relationshipofdroughtfrequency.pdf

Mishra, A. K., & Singh, V. P. (2010). A review of drought concepts. *Journal of hydrology*, *391*(1-2),202-216. https://www.sciencedirect.com/science/article/pii/S0022169410004257

Mustafa, E. K., Co, Y., Liu, G., Kaloop, M. R., Beshr, A. A., Zarzoura, F., & Sadek, M. (2020). Study for predicting land surface temperature (LST) using landsat data: a comparison of four algorithms. *Advances in Civil Engineering*, *2020*(1), 7363546. https://onlinelibrary.wiley.com/doi/abs/10.1155/2020/7363546

Naresh Kumar, M., Murthy, C. S., Sesha Sai, M. V. R., & Roy, P. S. (2009). On the use of Standardized Precipitation Index (SPI) for drought intensity assessment. *Meteorological Applications: A journal of forecasting, practical applications, training techniques and modelling*, *16*(3),381-389. https://rmets.onlinelibrary.wiley.com/doi/abs/10.1002/met.136

Nuskiya, M. H. F., Sawjanya, S., & Hewapathirana, I. S. A. (2025). Geospatial analysis of forest cover change and biodiversity loss in Batticaloa District. Wildlanka, 13(2), 211–220. https://www.researchgate.net/profile/Nuskiya-Hassan/publication/392367186_

Seiler, R. A., Kogan, F., & Sullivan, J. (1998). AVHRR-based vegetation and temperature condition indices for drought detection in Argentina. *Advances in Space Research*, *21*(3), 481-484. https://www.sciencedirect.com/science/article/pii/S0273117797008843

Srimali, A., Gunawardhana, L., Bamunawala, J., Sirisena, J., & Rajapakse, L. (2025). Impact of Spatio-Temporal Variability of Droughts on Streamflow: A Remote-Sensing Approach Integrating Combined Drought Index. *Hydrology*, *12*(6), 142. https://www.mdpi.com/2306-5338/12/6/142

Sun, D., & Kafatos, M. (2007). Note on the NDVI-LST relationship and the use of temperature-related drought indices over North America. *Geophysical research letters*, *34*(24). https://agupubs.onlinelibrary.wiley.com/doi/abs/10.1029/2007GL031485

Sun, N. S., Chen, Q., & Liu, F. G. (2022). Vegetation Health Index 1-km Grid Dataset in Yellow River–Huangshui River Valley (2000–2020). *J. Glob. Change Data Discov*, *4*, 589-596. https://www.geodoi.ac.cn/WebEn/HTML_INFO.aspx?Id=1011b162-3bb4-476a-bd3f-abfe690515ec

Survey Department of Sri Lanka. (2022). *Surveyor General's performance report for the year 2022* (Expenditure Head No. 288). Government of Sri Lanka. https://www.parliament.lk/uploads/documents/paperspresented/1691572282082840.pdf

Trenberth, K. E., Dai, A., Van Der Schrier, G., Jones, P. D., Barichivich, J., Briffa, K. R., & Sheffield, J. (2014). Global warming and changes in drought. *Nature Climate Change*, *4*(1), 17-22. https://www.nature.com/articles/nclimate2067

Venkatesh, K., John, R., Chen, J., Jarchow, M., Amirkhiz, R. G., Giannico, V., ... & Yuan, J. (2022). Untangling the impacts of socioeconomic and climatic changes on vegetation greenness and productivity in Kazakhstan. *Environmental Research Letters*, *17*(9), 095007. https://iopscience.iop.org/article/10.1088/1748-9326/ac8c59/meta

Vicente-Serrano, S. M., Beguería, S., Lorenzo-Lacruz, J., Camarero, J. J., López-Moreno, J. I., Azorin-Molina, C., ... & Sanchez-Lorenzo, A. (2012). Performance of drought indices for ecological, agricultural, and hydrological applications. *Earth Interactions*, *16*(10), 1-27. https://journals.ametsoc.org/view/journals/eint/16/10/2012ei000434.1.xml

Walawe Durage, K. V. N. (2023). *Forest change mapping using remote sensing and Google Earth Engine* (Doctoral dissertation, The University of Waikato). https://researchcommons.waikato.ac.nz/entities/publication/ff8b5dad-2eec-429b-b998-ad2025e9072e

World Bank. (2021). *Climate Risk Country Profile: Sri Lanka*. World Bank Group. https://openknowledge.worldbank.org/entities/publication/38364ccd-484b-5288-81a9-0a362a2fdfcc

Zahir, I. L. M., Nuskiya, M. H. F., Sangasumana, V. P., Iyoob, A. L., & Ameer, M. L. F. (2024). Monitoring urban green space using remote sensing derived-vegetation indices in Colombo District, Sri Lanka. *Procedia Computer Science*, *236*, 248-256. https://www.sciencedirect.com/science/article/pii/S1877050924010445

Zahir, I. L. M., Suthakaran, S., Iyoob, A. L., Nuskiya, M. H. F., & Fowzul Ameer, M. L. (2025). Application of Geospatial Technology for Disaster Risk Reduction Using Machine Learning Algorithm and OpenStreetMap in Batticaloa District, Eastern Province, Sri Lanka. *Artificial Intelligence in Remote Sensing for Disaster Management*, 161-183. https://onlinelibrary.wiley.com/doi/abs/10.1002/9781394287222.ch9

Zhang, H., Yin, G., & Zhang, L. (2022). Evaluating the impact of different normalization strategies on the construction of drought condition indices. *Agricultural and Forest Meteorology*, *323*,109045. https://www.sciencedirect.com/science/article/pii/S0168192322002349

Zhang, W., Jin, F. F., Zhao, J. X., Qi, L., & Ren, H. L. (2013). The possible influence of a nonconventional El Niño on the severe autumn drought of 2009 in Southwest China. *Journal of Climate*, *26*(21), 8392-8405. https://journals.ametsoc.org/view/journals/clim/26/21/jcli-d-12-00851.1.xml

Zhou, X., Wang, P., Tansey, K., Ghent, D., Zhang, S., Li, H., & Wang, L. (2019). Drought monitoring using the Sentinel-3-based multiyear vegetation temperature condition index in the Guanzhong plain, China. *IEEE journal of selected topics in applied earth observations and remote sensing*, *13*, 129-142. https://ieeexplore.ieee.org/abstract/document/8920222/